SCIENCE CHINA
Chemistry

• ARTICLES •

June 2015 Vol.58 No.6: 1005–1012
doi: 10.1007/s11426-014-5297-2

Tunable supramolecular hydrogels from polypeptide-PEG-polypeptide triblock copolymers

Xiaohui Fu[1], Yong Shen[1], Yinan Ma[1], Wenxin Fu[1*] & Zhibo Li[1,2*]

[1]*Laboratory of Polymer Physics and Chemistry; Institute of Chemistry, Chinese Academy of Sciences, Beijing 100190, China*
[2]*School of Polymer Science and Engineering, Qingdao University of Science and Technology, Qingdao 266042, China*

Received September 25, 2014; accepted October 13, 2014; published online January 21, 2015

A series of ABA triblock copolymers of poly(γ-(2-methoxy ethoxy)esteryl-glutamate)-block-poly(ethylene glycol)-block-poly(γ-(2-methoxy ethoxy)esteryl-glutamate) with poly(ethylene glycol) as middle hydrophilic B block and oligo(ethylene glycol)-functionalized polyglutamate (poly-*L*-EG_2Glu) as terminal A blocks were prepared via ring-opening polymerization of EG_2Glu *N*-carboxyanhydride (NCA). The resulting P(EG_2Glu)-*b*-PEG-*b*-P(EG_2Glu) triblocks can spontaneously form hydrogels in water. The intermolecular hydrogen bonding interactions between polypeptides blocks were responsible for the formation of gel network structure. These hydrogels displayed shear-thinning and rapid recovery properties, which endowed them potential application as injectable drug delivery system. The mechanical strength of hydrogels can be modulated by copolymer composition, molecular weight and concentrations. Also, it was found that the hydrogels' strength decreased with temperature due to dehydration of polypeptide segments. Atomic force microscopy and scanning electron microscopy images revealed that these hydrogels were formed through micelle packing mechanism. Circular dichroism and Fourier transform infrared spectroscopy characterizations suggested the poly-*L*-EG_2Glu block adopted mixed conformation. A preliminary assessment of drug release *in vitro* demonstrated the hydrogels can offer a sustained release of doxorubicin (DOX) and the release rate could be controlled by varying chemical composition.

hydrogel, polypeptide, *N*-carboxyanhydride (NCA), ring-opening polymerization (ROP), drug delivery

1 Introduction

Hydrogels have attracted considerable interest for their promising biomedical applications in controlled release and tissue engineering [1–4]. Compared with traditional polymer hydrogels, polypeptide-based hydrogels have the advantages of inherent biodegradability and biocompatibility. Also, the secondary structures of polypeptides offer additional factors to tune hydrogels' properties and functionalities [5]. For example, peptide amphiphiles (PAs), which consist of a hydrophobic alkyl chain and a hydrophilic peptide segment, were demonstrated a promising biomaterial for constructing various functional hydrogels [6,7].

However, PA materials were made by solid-phase peptide synthesizers, which involved multistep synthesis and tedious purification. Controlled ring-opening polymerization (ROP) of *N*-carboxyanhydride (NCA) is an alternative way to prepare polypeptide materials [8–11]. Also, polypeptides via ROP of NCAs can be used to make stimuli-responsive hydrogels [5,12]. For example, Jeong group [13–15] reported a series of thermal-sensitive hydrogels based on PEG and polyalanine. Chen *et al*. [16] demonstrated that PEG-*b*-poly(alkyl-*L*-glutamate) copolymers displayed micelle-assembled thermal-sensitive hydrogels. Heise and coworkers [17] reported that PEG-*b*-oligotyrosine copolymer formed thermal-responsive hydrogels at a very low concentration. We showed that diblock copolymer comprising PEG and poly(*L*-EG_4-SS-Cys) displayed thermal-responsive and irreversible sol-gel transition in water, which

*Corresponding authors (email: fuwenxin@iccas.ac.cn; zbli@iccas.ac.cn)

also can be used as potential reduction-responsive injectable hydrogel [18]. Very recently, our group [19,20] showed that alkyl-poly-*L*-EG2Glu amphiphiles and PEG-*b*-poly-*L*-EG_2-Glu diblock copolymers with specific compositions could spontaneously form hydrogels. Our work demonstrated that methoxy diethylene glycol functionalized polyglutamate, i.e., poly-*L*-EG_2Glu, had unique amphiphilic characteristics, which allowed desirable control over hydrogen bonding as well as assembly structures.

In addition to PA type materials and PEG-polypeptide diblock, linear ABA triblock copolymers, which are composed of a hydrophilic B block and hydrophobic A blocks, can also be employed to make different hydrogels [21,22]. For example, Jeong *et al*. [14,23] reported that ABA triblock with polypeptide as the A block can form reverse thermal gels. Considering the unique amphiphilic characteristic of poly-*L*-EG_2Glu, we herein reported the synthesis of P(EG_2Glu)-*b*-PEG-*b*-P(EG_2Glu) ABA type triblock copolymers (Scheme 1). Depending on the composition and molecular weight, these copolymers could spontaneously form hydrogels at room temperature, which showed tunable mechanical strength, shear-thinning and rapid recovery properties. We also examined the obtained hydrogels as controlled release system for doxorubicin (DOX).

2 Experimental

2.1 Synthesis of ABA triblock copolymers

The terminal hydroxyl groups of poly(ethylene glycol) (HO-PEG-OH, M_n=6 or 10 kDa) were converted into amine groups by firstly conjugation with N_α-tertbutyloxy-carbonyl-*L*-phenylalanine (Boc-Phe-OH) followed by deprotection of Boc group [24]. Typically, HO-PEG_{136}-OH (7.93 g, 1.32 mmol) and Boc-Phe-OH (3.50 g, 13.20 mmol) were dissolved in anhydrous dichloromethane (200 mL) at 0 °C. Dicyclohexylcarbodiimide (2.72 g, 13.20 mmol) and 4-dimethylaminopyridine (0.16 g, 1.32 mmol) were then added to the solution, and the reaction mixture was stirred at 0 °C for about 2 h and overnight at ambient temperature. After removing *N*,*N*′-dicyclohexylurea and washing, white solid products were obtained with 86% yield. Subsequently, the Boc groups were removed using excess trifluoroacetic acid/dichloromethane mixture. After purification, the diamine-functionalized PEG macroinitiator (NH_2-Phe-PEG_{136}-Phe-NH_2) was obtained with about 89% yield.

The synthesis and purification of γ-(methoxy ethoxy) esteryl-glutamate *N*-carboxyanhydride (EG_1Glu NCA) and γ-(2-methoxy ethoxy)esteryl-glutamate *N*-carboxyanhydride (EG_2Glu NCA) followed previously reported procedures [25]. The ABA triblock was prepared via ROP of EG_xGlu NCA using NH_2-Phe-PEG-Phe-NH_2 as initiator in *N*,*N*-dimethylformamide at 40 °C for 3 d. The consumption of NCA was confirmed by Fourier transform infrared spectroscopy (FTIR). The sample mixtures were precipitated into ethyl ether twice, collected by centrifugation, and dried in vacuum to yield a white solid. The yield was between 71% and 83%.

2.2 Rheology characterization

Copolymer samples were dispersed in deionized water to form hydrogels, which were equilibrated overnight at 20 °C. Rheology experiments were conducted on an Anton Paar-

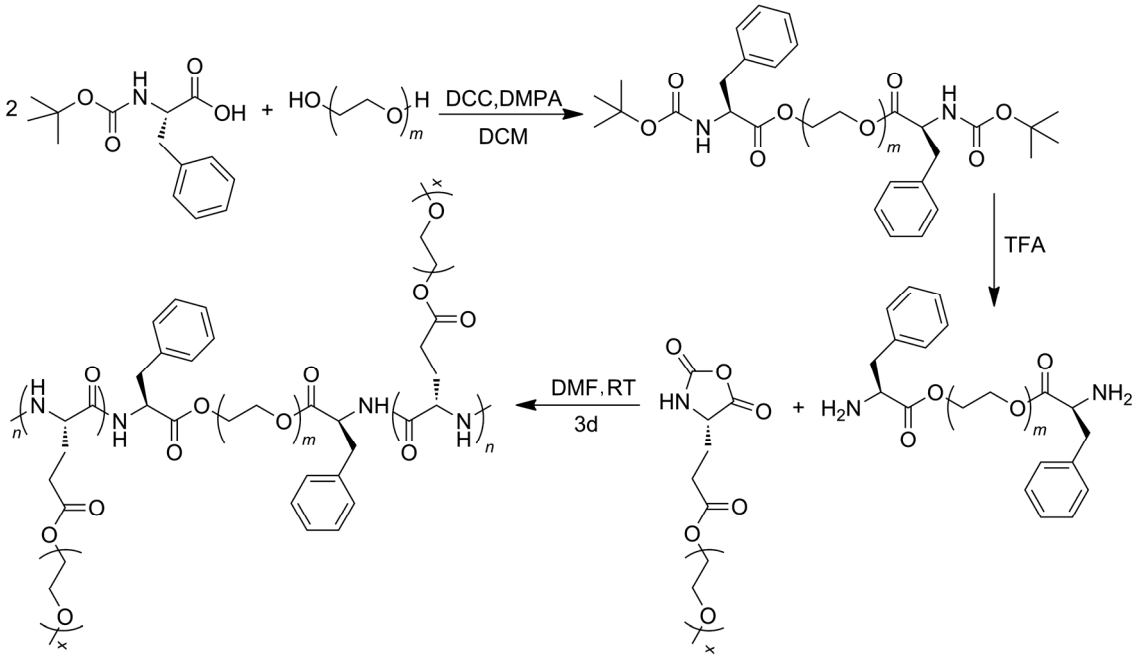

Scheme 1 Synthetic routes to ABA triblock copolymers.

Modular Compact Rheometer (MCR 502) with 25 mm diameter cone-plate geometry and 0.5 mm gap distance. The rheometer was equilibrated at predetermined temperature prior to loading sample. Low viscosity mineral oil was used to cover the sides of the plate to minimize water evaporation. Strain (γ_0) sweep experiments were performed to determine the linear viscoelastic regime (ω=6 rad/s, 20 °C). The frequency sweep (ω) was performed from 0.1 to 100 rad/s with a constant shear strain of 0.4%. Dynamic time sweep experiments were performed with ω=6.0 rad/s and γ_0=0.4%. The measurements of storage modulus (G') and loss modulus (G'') of hydrogels were made as a function of time and temperature from 20 to 60 °C with a heating rate of 0.5 °C/min. The extreme rotation shear was applied to disrupt the hydrogel at ω=6.0 rad/s, γ_0=60% for 600 s. Once the shear ceased, the dynamic viscoelastic properties (G' and G'') were immediately monitored over time in a subsequent dynamic time sweep.

2.3 Controlled release of DOX

DOX was used as a model drug for controlled release experiments. DOX·HCl was dissolved in deionized water and the pH was adjusted to about 9.6 with 0.1 mol/L NaOH. The DOX was collected by centrifugation, washed with distilled water 3 times, and followed by lyophilization in the dark. The controlled release behaviors of DOX were investigated following a literature procedure [17,26]. Hydrogels containing DOX (2 mg/mL) were prepared. A total of 150 mg hydrogel sample (c=80 mg/mL) with 2 mg/mL DOX was placed in each of three 5 mL glass vials, which was sonicated for 30 min and equilibrated at room temperature overnight before adding 2 mL phosphate buffer solution (0.01 mol/L, pH 7.4). The mixtures were allowed to incubate at predetermined temperature while shaking at 100 r/min for the duration of release study. The top buffer solution was isolated and replenished with fresh buffer solution. The isolated solution was then subject to DOX concentration determination. All studies were performed in triplicate, and the averaged results were reported. The DOX content was determined from UV-Vis spectroscopy at 485 nm using the standard curve method.

3 Results and discussion

3.1 Synthesis of ABA triblock copolymers

The NH_2-Phe-PEG-Phe-NH_2 macroinitiator was synthesized by the direct coupling between HO-PEG-OH and Boc-Phe-OH followed by deprotection of Boc groups. The chemical structures of Boc-Phe-PEG-Phe-Boc and NH_2-Phe-PEG-Phe-NH_2 were confirmed by ^{1}H NMR spectra (Figures 1(a) and S1(a), Supporting Information online). The resonances at 3.5–3.9, 1.4, and 7.2–7.4 ppm are attributed to protons of methylene groups in PEG, methyl in Boc-protective groups, and phenyl in phenylalanine, respectively (Figure 1(a-I)). The successful deprotection of the Boc group was verified by disappearance of the methyl peak in Boc groups (1.4 ppm, Figure 1(a-II)). The P(EG_2Glu)-*b*-PEG-*b*-P(EG_2Glu) triblock copolymers were synthesized by ROP of *L*-EG_2Glu NCA using NH_2-Phe-PEG-Phe-NH_2 as macroinitiator (Scheme 1). A series of triblock copolymers were obtained by varying the NCA to macroinitiator ratio (Table 1). Figure 1(a-III) shows the ^{1}H NMR spectrum of P(EG_2Glu)-*b*-PEG_{136}-*b*-P(EG_2Glu) (P6-1), which is in great agreement with expected structure. Using PEG as the reference, we compared the integration areas of ethylene glycol protons and the methoxy groups at 3.30–4.0 ppm and the β-methylene group at 2.0–2.7 ppm to determine the degree of polymerization (DP) of the poly-EG_2Glu block. Figures 1(b) and S1(b) compare the SEC traces of the NH_2-Phe-PEG-Phe-NH_2 and triblock copolymers. Apparently, the ABA triblock shifted to low elution volume indicating successful incorporation of poly-*L*-EG_2Glu segment. Although all ABA triblock copolymers displayed a shoulder peak at high molecular regime, the triblocks still had relatively narrow molecular weight distribution, which indicated controlled ROP of NCAs. The shoulder peak was most likely caused by coupling of PEG precursor. The corresponding molecular parameters are summarized in Table 1. Note that samples P6-1, P6-1(R), and P10-1 or samples P6-2 and P10-2 had similar polypeptide chain lengths, which help understanding the effects of molecular weight and composition on the gelation properties of copolymers.

Table 1 Molecular parameters of ABA triblock copolymers

Entry	Monomer [a]	Initiator	Polydispersity index (PDI) [b]	DP [c]	CGC [d]
P6-1	15 EG_2Glu NCA	NH_2-Phe-PEG_{136}-Phe-NH_2	1.09	12	4 wt%
P6-2	30 EG_2Glu NCA	NH_2-Phe-PEG_{136}-Phe-NH_2	1.08	18	3 wt%
P6-1(R)	7.5 EG_1Glu NCA:7.5 EG_2Glu NCA	NH_2-Phe-PEG_{136}-Phe-NH_2	1.10	13	4 wt%
P10-1	15 EG_2Glu NCA	NH_2-Phe-PEG_{227}-Phe-NH_2	1.07	12	4 wt%
P10-2	30 EG_2Glu NCA	NH_2-Phe-PEG_{227}-Phe-NH_2	1.12	19	4 wt%

a) Number indicates monomer/initiator ratio; b) determined by tandem size exclusion chromatography/laser light scattering (SEC/LLS); c) determined from ^{1}H NMR; d) determined by inverting tube method.

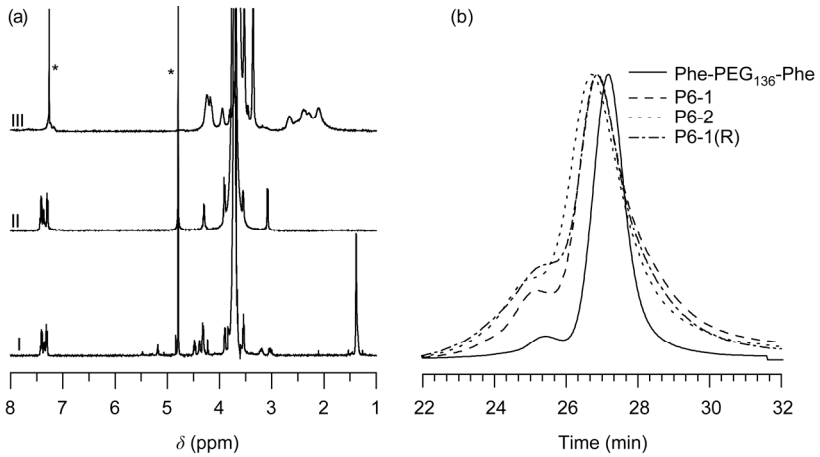

Figure 1 (a) ^{1}H NMR spectra of (I) Boc-Phe-PEG$_{136}$-Phe-Boc, (II) Phe-PEG$_{136}$-Phe in D_2O, and (III) P6-1 in $CDCl_3$/CF_3COOD (*v*/*v*, 1:1); (b) SEC traces of NH_2-Phe-PEG$_{136}$-Phe-NH_2 and triblock copolymers P6-1, P6-2, and P6-1(R).

3.2 Hydrogel characterization

All five samples in Table 1 can spontaneously form hydrogel in water at relatively low concentrations (Figure S7(a)). The critical gelation concentration (CGC) was determined by the inverting tube method (Table 1). The CGC for most samples was about 4 wt% except sample P6-2, which had CGC=3 wt%. The lower CGC of sample P6-2 was probably due to the relatively longer poly-*L*-EG$_2$Glu block and shorter PEG block compared with other samples [20].

The gel properties were characterized by rheology measurements. The dynamic strain sweep was conducted in the strain range of 0.01%–100% with $\omega = 6$ rad/s at 20 °C (Figure 2(a) and Figures S3(b)–S6(b)). The G' in the linear viscoelastic region was approximately one order of magnitude larger than the G'', indicating solid gel status. All hydrogels displayed clear gel-sol transition under large strain except sample P10-1, which was a weak and soft hydrogel (Figure S5(b)). Also, hydrogels of P6-1, P6-1(R), P6-2, and P10-2 could recover rapidly from sol to gel upon cease of shearing as shown in Figure 2(b). All four samples recovered to gel status upon stopping shearing within minimum switching time, ca. 10 s. For example, hydrogels of P6-1, P6-1(R), P6-2, and P10-2 recovered 77%, 80%, 69%, and 67% of its original strength within 10 s, respectively. Then, these hydrogels progressively regained their original strength and reached 97% (P6-1), 91% (P6-1(R)), 74% (P6-2), and 82% (P10-2) recovery within 10 min. Such shear-thinning and rapid recovery properties made these hydrogels promising candidates for injectable drug delivery system.

Frequency sweep measurements showed that the gel strength increased with concentration (Figures S2(a)–S6(a)). Given the same concentration, the hydrogel strength increased with the molecular weight of poly-*L*-EG$_2$Glu block, but decreased with chain length of middle PEG block (Figure 2(a)). At 5 wt%, the corresponding modulus increased from 38 to 175 Pa and to 3100 Pa for samples P6-1, P6-1(R), and P6-2, respectively. Interestingly, increase in the hydrophobicity of polypeptide block, that is, addition of more hydrophobic *L*-EG$_1$Glu monomers, also caused an increase in hydrogel modulus given similar overall molecular weight. The modulus for P10-1 and P10-2 increased from 12 to 60 Pa at 5 wt% concentration. These results suggested that the mechanical strength can be modulated from 1 to 3000 Pa by simply adjusting concentrations and sample compositions to meet specific application requirements.

In contrast to other thermal-responsive hydrogels, the P(EG$_2$Glu)-*b*-PEG-*b*-P(EG$_2$Glu) triblock hydrogels displayed temperature-induced weakening of mechanical strength (Figure 2(d)). For example, P6-1(R) formed solid gel at 5 wt% at 20 °C. As the temperature gradually increased from 20 to 60 °C, the G' decreased from 120 Pa to around 5 Pa, while the G'' did not show obvious change with temperature variation (Figure 2(d)). Similar results were observed for other samples. As illustrated in Figure S7, hydrogel of sample P6-1 underwent a clear gel-sol transition upon heating from room temperature to 60 °C. The results may be attributed to the destruction of delicate hydrophilic/hydrophobic balance and the regular hydrophobic packing.

3.3 Structure characterization

The morphology of the copolypeptide hydrogels was characterized using atomic force microscopy (AFM) and scanning electron microscopy (SEM) (Figures 3 and S8–S11). AFM revealed packed micellar structures within hydrogel sample, which indicated a percolating network connected by spherical micelles (Figure 3(a)). Samples for the SEM characterization were treated with liquid nitrogen followed by lyophilization to preserve the hydrogel structures. SEM images also confirmed the porous network structure (Figure 3(b)). These results are different from the hydrogel structures of PEG-*b*-poly-*L*-EG$_2$Glu or alkyl-poly-*L*-EG$_2$Glu, in

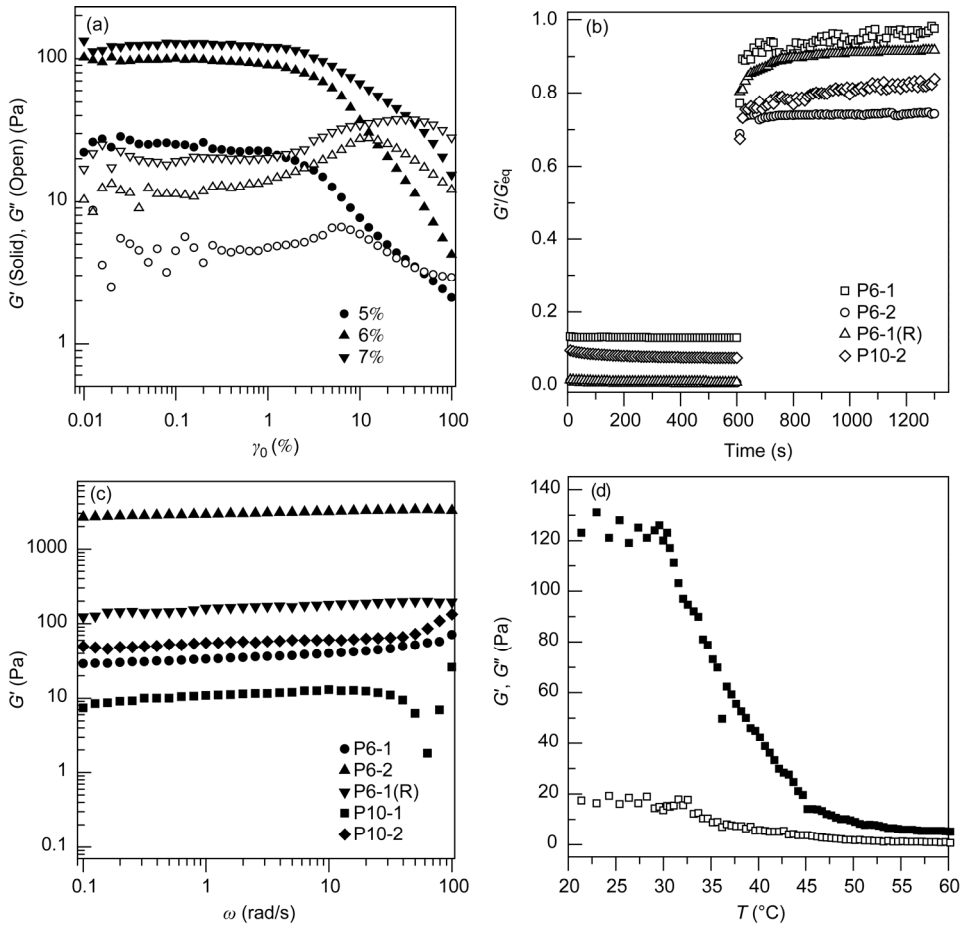

Figure 2 (a) G' (solid symbols) and G'' (open symbols) as a function of strain for P6-1 hydrogel at different concentrations with ω=6.0 rad/s; (b) G'/G'_{eq} as a function of time for P6-1, P6-2, P6-1(R) and P10-2 hydrogels, which were sheared at ω=6.0 rad/s and γ_0=60% for 600 s before switching to small strain (ω=6.0 rad/s and γ_0=0.4%). G' was normalized to the equilibrium value (G'_{eq}); (c) plots of storage modulus G' for hydrogels P6-1 (●), P6-2 (▲), P6-1(R) (▼), P10-1 (■), and P10-2 (◆) at a concentration of 5 wt%; (d) G' (■) and G'' (□) of the P6-1(R) hydrogel as a function of temperature at 5 wt%.

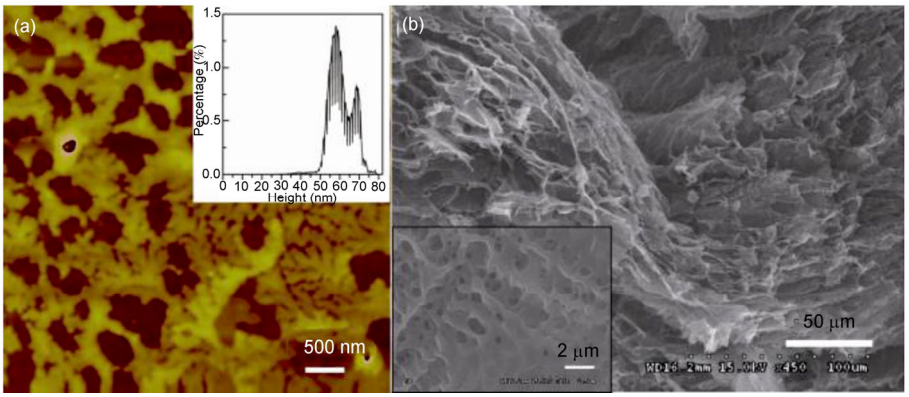

Figure 3 (a) AFM image of P10-2 hydrogel with c=5 wt% (the inset is the height histogram); (b) SEM image of P10-2 hydrogel (5 wt%) after lyophilization (the inset is a magnified SEM image).

which the hydrogel networks were formed by nanoribbon assemblies [19,20].

3.4 Conformational analysis

To understand polypeptide conformation within the formed micelles, circular dichroism (CD) spectroscopy was performed to analyze the samples' conformation. As shown in Figure 4, all samples exhibited two negative bands around 208 and 222 nm and one positive band near 190 nm, which are characteristics of α-helical conformation [27]. Apparently, the corresponding molar ellipticity increased with DP

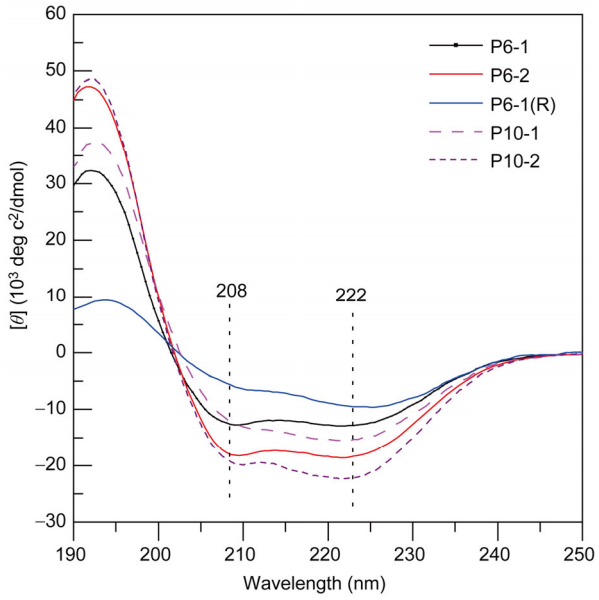

Figure 4 CD spectra of P(EG$_x$Glu)-*b*-PEG-*b*-P(EG$_x$Glu) at 25 °C. The concentration is 0.5 mg/mL.

of poly-*L*-EG$_2$Glu block. For example, as the DP of poly-*L*-EG$_2$Glu block increased from 12 (P6-1) to 18 (P6-2) with same PEG (6 kDa) middle block, the helical content increased from 41% to 55%. Similarly, P10-1 and P10-2 with same PEG (10 kDa) middle block had helicities of 47% and 65%, respectively. The above results suggested that longer poly-*L*-EG$_2$Glu preferred to form more helical structures [28]. On the other hand, the helical content also increased with the molecular weight of PEG middle block given similar DP of poly-*L*-EG$_2$Glu block. For example, sample P10-1 had higher helicity than that of P6-1. A possible reason is that the longer PEG middle block is more hydrophilic, which prevented the formation of β-sheet [15,20]. Also, P6-1(R), which has similar DP and PEG molecular weight to P6-1, had lower helical content. This result suggested that the α-helix content decreases when the β-sheet favorable monomer (*L*-EG$_1$Glu) was introduced [25].

The samples' conformation at solid state was characterized using FTIR. As shown in Figure 5, all the five samples had two absorption bands at 1654 and 1625 cm^{-1} (amide I band), which revealed the coexistence of α-helix and β-strand structures. The strong carbonyl absorption at 1654 cm^{-1} (amide I) and the N–H absorption at 1549 cm^{-1} (amide II) indicated predominate α-helical conformation. This contrasts with the conformation of alkyl-poly-*L*-EG$_2$Glu amphiphiles, in which β-sheet was the major conformation [19,20]. We assumed that the long PEG middle blocks destabilized the β-sheet structure of the peptide blocks. These results were consistent with CD measurements discussed above, suggesting that the increase of PEG length is unfavorable for forming β-sheet conformation.

Temperature-varied CD measurements were applied to investigate the temperature influences on polypeptide conformation for samples P6-2 and P6-1(R). Figure S12 shows the corresponding CD spectra at different temperatures in heating ramp. Apparently, both samples did not show obvious conformation changes upon temperature increase. Cooling scan of the same solution showed negligible change in its secondary structure (Figure S13).

It was known that poly-EG$_2$Glu block had amphiphilic nature. Its solution properties had strong dependence on molecular weight [28]. When the DP was higher than 60, it was thermal responsive. When the DP was lower than 46, it was amphiphilic since the polypeptide chain preferred to form aggregates via intermolecular hydrogen bonding [19,20,28,29]. Therefore, for P(EG$_2$Glu)-*b*-PEG-*b*-P(EG$_2$Glu) triblock, it was mainly the hydrogen bonding interactions of poly-*L*-EG$_2$Glu blocks that contributed to the formation of hydrogels. At low concentration, the ABA triblock copolymers mainly assembled into flower-like micelles. When the polymer concentration is efficiently high, the micelles will start to contact, and the central PEG block

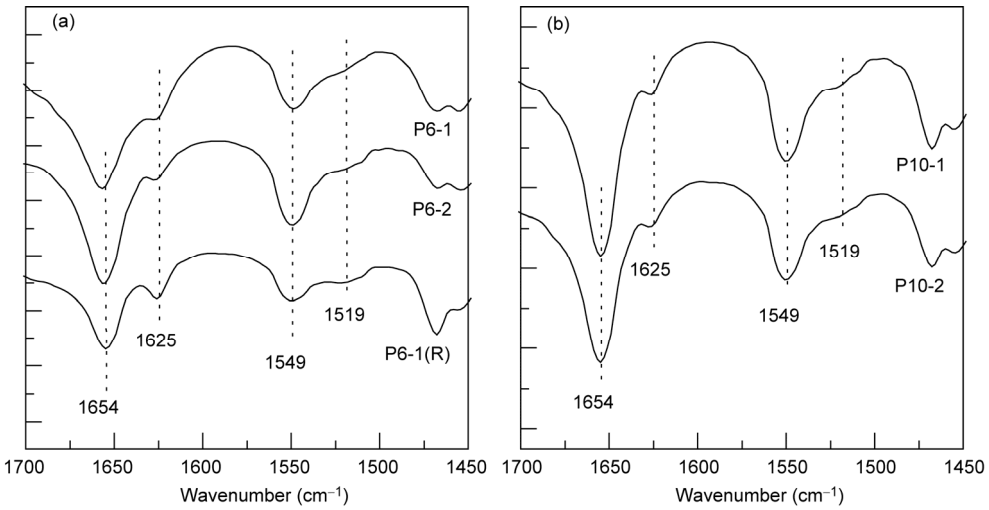

Figure 5 FTIR spectra of (a) P(EG$_x$Glu)-*b*-PEG$_{136}$-*b*-P(EG$_x$Glu) and (b) P(EG$_2$Glu)-*b*-PEG$_{227}$-*b*-P(EG$_2$Glu) in the solid state.

will form bridges among micelle cores, which lead to solid micelle packing and ultimately to three-dimensional networks [30]. Since the poly-*L*-EG_2Glu block was not strongly hydrophobic, the intermicellar exchange of poly-*L*-EG_2Glu block was not thermodynamically difficult. Hence, we inferred that the temperature-induced decrease in gel strength could be attributed to two possible reasons. First, the micellar aggregates shrank with the increase of temperature due to the destruction of hydrogen bonds between OEG side chains and water [25]. Second, the significant portion of PEG central blocks formed loops in the corona (flower micelles) for their partial dehydration, which resulted in rather weak bridges among micelles [31,32]. The two forces cooperatively disturbed the delicate hydrophilic/hydrophobic balance and the regular hydrophobic packing, leading to the disruption of the physical network structures.

3.5 Drug-loaded hydrogels and controlled release behavior

As a preliminary study on the bioapplications of the hydrogels, we demonstrated the controlled release of DOX from the gel matrix. In this study, after the formation of DOX-loaded hydrogels (8 wt% hydrogels), the drug release properties of the peptide hydrogels were investigated at 37 °C and the corresponding release profiles were exhibited in Figure 6. Clearly, all cases had an initial quick release of DOX and the initial release rates were essentially the same within the first 24 h (Figure 6). It appeared that the diffusion of DOX from the hydrogels to the release media was the dominant process and the dissolution rates of hydrogels had little contribution to the release of DOX for the first day [33]. The reason was most likely that the size of DOX is smaller than the mesh size of the micellar hydrogels of all the samples. However, the releases of P6-1, P10-1, and P10-2 were sustained only for 7 days due to the gradual erosion of the hydrogels. The accumulated DOX releases after 7 days followed the order P6-1 (54%) ≈ P10-1 (54%) > P10-2 (40%) > P6-2 (33%) > P6-1(R) (28%). Interestingly, the duration of releases from P6-2 and P6-1(R) hydrogels was significantly extended to 20 days under similar release conditions *in vitro*. It seemed that the rate of erosion was higher for more hydrophilic samples. That is because the increased hydrophilicity facilitates the diffusion of water and thus enhances erosion of the polymers [34]. These results indicated that the drug release rate of the DOX-loaded hydrogels can be adjusted by the chemical composition of the copolypeptides.

4 Conclusions

In summary, a series of ABA triblock copolymers were synthesized in different compositions via the ROP of NCAs using NH_2-PEG-NH_2 as macroinitiator. These copolymers could spontaneously form hydrogels at room temperature and the gel strength could be enhanced with increasing concentration and length of polypeptide blocks, as well as incorporation of more hydrophobic *L*-EG_1Glu monomer. The triblock hydrogels had shear-thinning and rapid recovery properties, which were critical features for injectable hydrogel. AFM and SEM results showed the hydrogels were composed of micelles. A preliminary assessment of drug release *in vitro* confirmed the hydrogels produced a sustained release of DOX and the release rate could be controlled by varying chemical composition. These peptide-based hydrogels may have potential application as injectable drug delivery system.

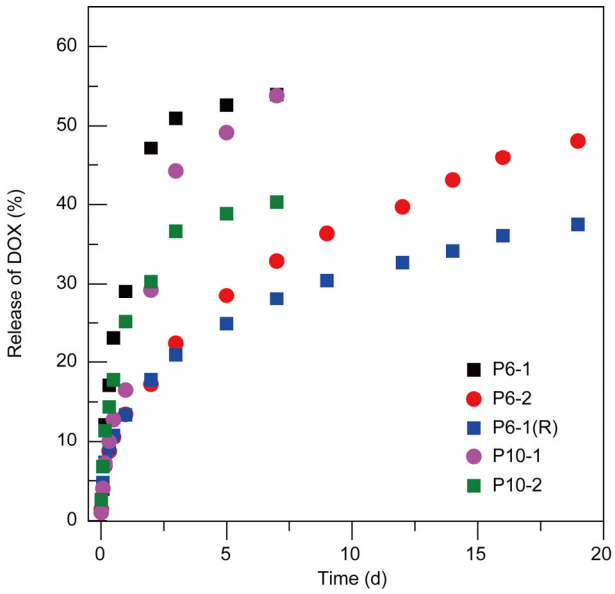

Figure 6 Cumulative release of DOX (%) over time from 8 wt% ABA micellar hydrogels at 37 °C.

Supporting Information

The supporting information is available online at chem.scichina.com and link.springer.com/journal/11426. The supporting materials are published as submitted, without typesetting or editing. The responsibility for scientific accuracy and content remains entirely with the authors.

This work was financially supported by the National Natural Science Foundation of China for Distinguished Young Scholar (51225306) and the CAS-CSIRO Cooperative Research Program (GJHZ1408).

1 Seliktar D. Designing cell-compatible hydrogels for biomedical applications. *Science*, 2012, 336: 1124–1128
2 Van Vlierberghe S, Dubruel P, Schacht E. Biopolymer-based hydrogels as scaffolds for tissue engineering applications: a review. *Biomacromolecules*, 2011, 12: 1387–1408
3 Vashist A, Vashist A, Gupta YK, Ahmad S. Recent advances in hydrogel based drug delivery systems for the human body. *J Mater Chem B*, 2014, 2: 147–166
4 Chen Z, Wang W, Guo L, Yu Y, Yuan Z. Preparation of enzymati-

cally cross-linked sulfated chitosan hydrogel and its potential application in thick tissue engineering. *Sci China Chem*, 2013, 56: 1701–1709
5 Zhang S, Li Z. Stimuli-responsive polypeptide materials prepared by ring-opening polymerization of alpha-amino acid *N*-carboxyanhydrides. *J Polym Sci, Part B: Polym Phys*, 2013, 51: 546–555
6 Hartgerink JD, Beniash E, Stupp SI. Self-assembly and mineralization of peptide-amphiphile nanofibers. *Science*, 2001, 294: 1684–1688
7 Cui H, Webber MJ, Stupp SI. Self-assembly of peptide amphiphiles: from molecules to nanostructures to biomaterials. *Biopolymers*, 2010, 94: 1–18
8 Deming TJ. Synthetic polypeptides for biomedical applications. *Prog Polym Sci*, 2007, 32: 858–875
9 Lu H, Wang J, Song ZY, Yin LC, Zhang YF, Tang HY, Tu CL, Lin Y, Cheng JJ. Recent advances in amino acid *N*-carboxyanhydrides and synthetic polypeptides: chemistry, self-assembly and biological applications. *Chem Comm*, 2014, 50: 139–155
10 Peng H, Chen WL, Kong J, Shen ZQ, Ling J. Synthesis of α-hydroxy-ω-aminotelechelic polypeptide from α-amino acid *N*-carboxyanhydrides catalyzed by alkali-metal borohydrides. *Chin J Polym Sci*, 2014, 32: 743–750
11 Yang WX, Wang LL, Zhu H, Xu RW, Wu YX. Synthesis of poly (glutamic acid-*co*-aspartic acid) via combination of *N*-carboxyanhydride ring opening polymerization with debenzylation. *Chin J Polym Sci*, 2013, 31: 1706–1716
12 Huang J, Heise A. Stimuli responsive synthetic polypeptides derived from *N*-carboxyanhydride (NCA) polymerisation. *Chem Soc Rev*, 2013, 42: 7373–7390
13 Choi YY, Joo MK, Sohn YS, Jeong B. Significance of secondary structure in nanostructure formation and thermosensitivity of polypeptide block copolymers. *Soft Matter*, 2008, 4: 2383–2387
14 Oh HJ, Joo MK, Sohn YS, Jeong B. Secondary structure effect of polypeptide on reverse thermal gelation and degradation of l/dl-poly (alanine)-poloxamer-l/dl-poly(alanine) copolymers. *Macromolecules*, 2008, 41: 8204–8209
15 Choi YY, Jang JH, Park MH, Choi BG, Chi B, Jeong B. Block length affects secondary structure, nanoassembly and thermosensitivity of poly(ethylene glycol)-poly(l-alanine) block copolymers. *J Mater Chem*, 2010, 20: 3416–3421
16 Cheng Y, He C, Xiao C, Ding J, Zhuang X, Huang Y, Chen X. Decisive role of hydrophobic side groups of polypeptides in thermosensitive gelation. *Biomacromolecules*, 2012, 13: 2053–2059
17 Huang J, Hastings CL, Duffy GP, Kelly HM, Raeburn J, Adams DJ, Heise A. Supramolecular hydrogels with reverse thermal gelation properties from (oligo)tyrosine containing block copolymers. *Biomacromolecules*, 2013, 14: 200–206
18 Ma Y, Fu X, Shen Y, Fu W, Li Z. Irreversible low critical solution temperature behaviors of thermal-responsive oegylated poly(l-cysteine) containing disulfide bonds. *Macromolecules*, 2014, 47: 4684–4689
19 Chen C, Wu D, Fu W, Li Z. Peptide hydrogels assembled from nonionic alkyl-polypeptide amphiphiles prepared by ring-opening polymerization. *Biomacromolecules*, 2013, 14: 2494–2498
20 Zhang S, Fu W, Li Z. Supramolecular hydrogels assembled from nonionic poly(ethylene glycol)-*b*-polypeptide diblocks containing oegylated poly-*l*-glutamate. *Polym Chem*, 2014, 5: 3346–3351
21 Ward MA, Georgiou TK. Thermoresponsive gels based on aba triblock copolymers: does the asymmetry matter? *J Polym Sci, Part A: Polym Chem*, 2013, 51: 2850–2859
22 Lin Z, Cao S, Chen X, Wu W, Li J. Thermoresponsive hydrogels from phosphorylated ABA triblock copolymers: a potential scaffold for bone tissue engineering. *Biomacromolecules*, 2013, 14: 2206–2214
23 Kim EH, Joo MK, Bahk KH, Park MH, Chi B, Lee YM, Jeong B. Reverse thermal gelation of paf-plx-paf block copolymer aqueous solution. *Biomacromolecules*, 2009, 10: 2476–2481
24 Bauri K, De P, Shah PN, Li R, Faust R. Polyisobutylene-based helical block copolymers with pH-responsive cationic side-chain amino acid moieties by tandem living polymerizations. *Macromolecules*, 2013, 46: 5861–5870
25 Chen C, Wang Z, Li Z. Thermoresponsive polypeptides from pegylated poly-*L*-glutamates. *Biomacromolecules*, 2011, 12: 2859–2863
26 Qu W, Chen S, Ren S, Jiang XJ, Zhuo RX, Zhang XZ. A bioreducible polypeptide for efficient gene transfection both *in vitro* and *in vivo*. *Chin J Polym Sci*, 2013, 31: 713–718
27 Greenfield NJ. Using circular dichroism spectra to estimate protein secondary structure. *Nat Protoc*, 2006, 1: 2876–2890
28 Zhang S, Chen C, Li Z. Effects of molecular weight on thermal responsive property of pegylated poly-*l*-glutamates. *Chin J Polym Sci*, 2013, 31: 201–210
29 Shen J, Chen C, Fu W, Shi L, Li Z. Conformation-specific self-assembly of thermo-responsive poly(ethylene glycol)-*b*-polypeptide diblock copolymer. *Langmuir*, 2013, 29: 6271–6278
30 Jeong B, Bae YH, Kim SW. Thermoreversible gelation of peg-plga-peg triblock copolymer aqueous solutions. *Macromolecules*, 1999, 32: 7064–7069
31 O'Lenick TG, Jiang X, Zhao B. Thermosensitive aqueous gels with tunable sol gel transition temperatures from thermo- and pH-responsive hydrophilic aba triblock copolymer. *Langmuir*, 2010, 26: 8787–8796
32 O'Lenick TG, Jin N, Woodcock JW, Zhao B. Rheological properties of aqueous micellar gels of a thermo- and pH-sensitive aba triblock copolymer. *J Phys Chem B*, 2011, 115: 2870–2881
33 Hamidi M, Azadi A, Rafiei P. Hydrogel nanoparticles in drug delivery. *Adv Drug Deliv Rev*, 2008, 60: 1638–1649
34 Kissel T, Li YX, Unger F. Aba-triblock copolymers from biodegradable polyester a-blocks and hydrophilic poly(ethylene oxide) b-blocks as a candidate for *in situ* forming hydrogel delivery systems for proteins. *Adv Drug Deliv Rev*, 2002, 54: 99–134